Bubble Behavior in a Horizontal Narrow Divergent Passage (One-Dimensional Approximate Analysis)

Manuscript for Heat Transfer Asia Reaserch

表題 BUBBLE BEHAVIOR IN A HORIZONTAL NARROW DIVERGENT PASSAGE (ONE-DIMENSIONAL APPROXIMATE ANALYSIS)

著者及所属 Junichi Ohta, Fujio Yamamoto, and Mitsuyuki Koketsu

Department of Mechanical Engineering, Faculty of Engineering

Fukui University, Japan

原報 Translated from Transaction of JSME (B) 62, 597, 1884-1890 (1996)

翻訳者名 by Junichi Ohta

Department of Mechanical Engineering, Faculty of Engineering,

Fukui University

及宛先 3-9-1, Bunkyo, Fukui-shi 910, JAPAN

Tel: +81-776-27-8792

Fax: +81-776-27-8748

E-mail ohta@fv.mech.fukui-u.ac.jp

ABSTRACT—This paper investigates behavior of a bubble which bridges a gap in a cross section of a horizontal narrow divergent passage under the Earth's gravity condition (1G) analytically. In a narrow passage, inertia forces are known to be small compared with viscous forces. Also, gravity force is not dominant for bubble behavior in a horizontal narrow passage. In this sense, the bubble behavior in the passage is similar to that under a microgravity condition. It is important to understand the bubble behavior in relation to separating gas from a gas-liquid two-phase flow and controlling a gas-liquid interface under a microgravity condition. A one-dimensional momentum equation for the bubble behavior is derived. The equation is arranged to an ordinary differential equation with respect to the upstream interfacial location and is solved. Analytical results are compared with experimental those. As a result, effects of gap size, bubble projected area, and divergent angle on the bubble behavior are explained qualitatively.

Key words: Bubble, Surface Tension, Microgravity, Meniscus, Hele-Shaw Cell, Separation, Narrow Space

1. INTRODUCTION

Recently, a two-phase flow loop, using a gas-liquid two-phase flow, has attracted attention as one of advanced thermal management technologies in a space station or a space base [(1), (2)]. In the thermal management device, control of the gas-liquid interface and separation of the gas from the gas-liquid two-phase flow are needed under a microgravity condition. It is important to understand the behavior of a bubble which bridges a cross section of a divergent passage for designing a flat type heat pipe, various connectors, and a device maintaining liquid with many parallel plates having narrow spaces. From the point of view of

the background, the purpose of a series of these studies is to clarify the behavior of the bubble that bridges the cross section of the horizontal divergent passage under a microgravity condition. This study is conducted under the Earth gravity condition. Inertia forces are known to be small compared with viscous forces [(3)], gravity force is not dominant in bubble behavior in a horizontal narrow passage under the 1-G condition. Hence, the bubble behavior in the passage under the 1-G is considered to be similar to that under a microgravity condition. There were studies on a gas-liquid interface behavior in a tube by Ichikawa [(4)], bubble behavior in a narrow passage [(5)], bubble behavior [(6)], a pump using surface tension under a microgravity condition [(7)]. However, a theoretical analysis such as the present study does not seem to be made.

In the authors' previous report [(8)], the observation and measurement were conducted in the same situation as the present study. It was found that the bubble moved to the larger cross section in the divergent passage and that effects of the projected bubble area, the gap size, and the divergent angle on the bubble behavior and the shape of the bubble were clarified by the experiments. In this report, one-dimensional momentum equation is derived and arranged to an ordinary differential equation with respect to an upstream interface. Substituting of an effective area ratio into the equation, analytical results are obtained and compared with the experimental those. The effective area ratio will be described in a subsequent report in detail.

NOMECRATURE

$A(x)$: A cross-sectional area of divergent passage at location x from the converging point (see Fig. 1)

F : Liquid area viewed from the top

k : Effective area ratio; The ratio of an area where a bubble is pressed against side wall to an effective bubble area which is viewed from the side (The definition is mentioned in section 2.1)

2. THEORETICAL ANALYSIS

2.1 An Effective Area Pressed against Side Wall by a Bubble

An experimental apparatus for the bubble behavior is referred to the authors' previous report [8] and is presented again as appendix in Fig. 7. When a side view of the bubble was observed using experimental apparatus C which was used and shown in Fig. 3 of the previous report [8], it appears as if the bubble touched the side wall of the spacers for passage. The pseudo-touch area looks like a black ellipse in the side view as shown in Fig. 1. However, the authors deduce from the followings, that a very thin liquid layer exists between the bubble and the side wall at the pseudo-touch area.

(1) A thin liquid film between the bubble and the upper plate could be recognized when the authors observed the bubble in the apparatus in Fig. 7 from appropriate angles.

(2) Ichikawa [4] measured behavior of a gas-liquid interface that was located in a horizontal glass tube. After the glass tube was dried by flowing dry gas through the tube for twenty minutes, experiments were carried out. The gas-liquid interface was pulled and moved by the surface tension. He found that the first and second data were distinct from each other. However, he reported that the reproducibility was obtained after repeating the experiment several times. He explained that a number of the liquid molecules would attach on the inside wall of the tube every experiment and the distribution of the molecules would become uniform after the several experiments, hence the solid surface would not affect the gas-liquid interface behavior.

The black ellipse in Fig. 1 represents an area where a bubble is pressed against the side wall. A variable of k denotes the ratio of the black ellipse to a rectangular area between x_1 and x_2 in the side view, i.e. [$h\ (x_2 - x_1) / \cos\ \phi$], in Fig. 1[**1]. Namely, the effective area where the

[**1] The variable of k was called the ratio of an area where a bubble touches the side wall to an area of the bubble in the side view in the previous report [8].

bubble is pressed against the side wall is expressed as [$kh(x_2 - x_1) / cos \phi$].

2.2 Discussion of Bubble and Liquid Transportation

A pressure difference at the gas-liquid interface of the bubble is considered to be given by the Laplace's equation [9], since the liquid velocity is considerably low. Hence, the pressure in the bubble, P_i, is higher than that for the surrounding liquid. As mentioned in section 2.1, part of the bubble is pressed against the side wall of the spacers for passage (see Fig. 7). The pressure in the bubble P_i is equal to that on the side wall surface, P_s, since the radius of curvature for the gas-liquid interface is infinity at the black ellipse in Fig. 1. Therefore, the bubble is pushed in the normal direction of the black ellipse area at a pressure of P_i by the side wall. It is considered that the side wall pushes the bubble, and then the bubble pushes the surrounding liquid, thus the bubble behaves like a piston which pushes the surrounding liquid. Because of the low liquid velocity, a pressure of the liquid in the vessel can be considered to be constant compared with the pressure difference between the bubble and the liquid, i.e. the liquid pressure difference between upstream and downstream of the bubble is negligible. Therefore, the component in the axial direction of the net force acting on the bubble F_d can be expressed by Eq. (1) [**2] using pressures in the bubble P_i, on the liquid downstream of the bubble P_o, and on the liquid upstream of the bubble P_o.

$$F_d = 2 \cdot \Delta P \cdot k \cdot h \cdot (x_2 - x_1)\tan\phi \tag{1}$$

where ΔP (= P_i -P_o) is the pressure difference between the bubble and the liquid.

2.3 Basic Equations

2.3.1 Momentum Equation

Based on the liquid motion in the divergent passage instead of the gas bubble motion, a momentum equation is derived for analyzing the bubble behavior. The reasons are as follows.

[**2] Even if the bubble touches the side wall, the component in the axial direction of the net external

It is expected to be difficult to solve the momentum equation for the bubble due to the small gas density compared with the liquid that. Also, the momentum equation for the bubble may cause the calculation to be unstable. The bubble behavior can be expressed as a one-dimensional model, assuming the followings.

(1) The bubble and the liquid can be regarded as incompressible fluids in the present condition. Change in the bubble volume was confirmed to be negligible along the passage by extra experiments.

(2) An average liquid velocity over a cross section is taken as the one-dimensional velocity, so that the average velocity is changed with cross-sectional area.

(3) An unsteady term on the outside of the divergent passage can be neglected, since the velocity is considerably lower than that inside the passage. Even if velocities in the outside of the divergent passage are taken as one velocity, such as the velocity at the exit of the passage, the difference between the results obtained by the assumption and those neglecting the outside velocity was confirmed to be negligibly small.

(4) Friction force is estimated based on the Poiseullie flow in an infinite parallel channel. The friction force is considered inside and outside the divergent passage. The effect of the friction will be discussed in section 3.1.

(5) Equation (1) is taken into account as a force acting on the liquid in Eq.(2). A value of k in Eq. (1) is provided by authors' another experiment.

(6) The liquid and the spacers are ethyl alcohol and acrylic resin, respectively. Referring to literature [10], the value of the contact angle between those is set at zero degree[**3].

(7) As mentioned in section 2.1, it is considered that the bubble is pressed against the side, upper, and lower walls and that a thin liquid film exists between the bubble and the walls. Hence, the boundary conditions between the bubble and the wall are the slip conditions. The authors believe that the surface tension does not appear in the momentum Equation (2)

---

force for the bubble can be expressed as the same form as Eq. (1) in section 2.2.

[**3] In the case that the contact angle is not zero, this analysis is not applicable directly.

explicitly, but it acts on the bubble in the form of Eq. (1).

(8) Based on the previous report's discussion [8], the liquid flows through the four corner gaps between the bubble and the inner wall of the passage are not taken into account in the shape and the size such as the present apparatus.

(9) Force caused by the pressure difference between the inlet and the outlet of the divergent passage is negligible compared with the forces, such as Eq.(1).

(10) Other forces are not included in this analysis.

Hence, the momentum equation for the liquid in the passage [**4] can be written as

$$\int_{x_0}^{x_u} \rho \frac{d^2x}{dt^2} A(x)dx + \int_{x_d}^{x_e} \rho \frac{d^2x}{dt^2} A(x)dx = 2 \cdot \Delta P \cdot k \cdot h \cdot (x_2 - x_1)\tan\phi - \iint_F \tau_w dF \qquad (2)$$

where x_0 , x_u , x_d , x_e , x_1, and x_2 denote as the passage inlet location, upstream interfacial location, downstream interfacial location, passage outlet location, side passage location pseudo-touching the upstream gas-liquid interface, and side passage location pseudo-touching the downstream gas-liquid interface, respectively. The definitions of the variables in this paper were presented in Nomenclature and in Fig.4 of the previous report [8]. The first and second terms on the left hand side of Eq. (2) are unsteady terms for liquid in the passage. The first term on the right hand side is a force that the bubble pushes on the liquid, the second term on the right hand side of Eq. (2) stands for a friction force on the parallel walls.

2.3.2 Continuity Equation

[**4] Since the momentum equation is derived for the regions of the inside and outside of the passage, momentum terms entering and coming out of the passage are excluded in Eq. (2).

$$A(x)\frac{dx}{dt} = A(x_u)\frac{dx_u}{dt} \tag{3}$$

where $$A(x) = 2\tan\phi \cdot x \cdot h \tag{4}$$

Hence, Eq. (3) can be expressed as

$$x\frac{dx}{dt} = x_u\frac{dx_u}{dt} \tag{5}$$

In the following sections, each term in the momentum equation will be rewritten with x_u , so that Eq. (2) will be arranged to an ordinary differential equation with respect to x_u

2.3.3 Unsteady Term for Liquid

Making use of Eqs. (3), (4), and (5), the first term on the left hand side of Eq. (2) becomes

$$2 \cdot \rho \cdot \tan\phi \cdot h \cdot \int_{x_0}^{x_u} \left[\left(\frac{dx_u}{dt}\right)^2 + x_u\frac{d^2x_u}{dt^2} - \left(\frac{x_u}{x}\right)\left(\frac{dx_u}{dt}\right)^2 \right] dx \tag{6}$$

where the variable x_u can come out of the integral in Eq. (6). The similar arrangement is made for the liquid block downstream of the bubble. After the two equations are integrated, the first and second terms on the left hand side of Eq. (2) now become

$$\begin{aligned} 2\rho \cdot \tan\phi \cdot h \Bigg[& \left\{ \left(\frac{dx_u}{dt}\right)^2 + x_u\frac{d^2x_u}{dt^2} \right\} (x_u - x_0) + x_u^2 \left(\frac{dx_u}{dt}\right)^2 \left(\frac{1}{x_u} - \frac{1}{x_0}\right) \\ & + \left\{ \left(\frac{dx_u}{dt}\right)^2 + x_u\frac{d^2x_u}{dt^2} \right\} (x_e - x_d) + x_u^2 \left(\frac{dx_u}{dt}\right)^2 \left(\frac{1}{x_e} - \frac{1}{x_d}\right) \Bigg] \end{aligned} \tag{7}$$

2.3.4 Force by the Bubble Acting on Liquid

The first term on the right hand side of Eq. (2) represents as follows:

$$2 \cdot \sigma \left[\frac{2}{h} + \frac{1}{R(x)} \right] (x_2 - x_1) k \cdot h \cdot \tan\phi$$

where the upstream radius of curvature R_u is taken as $R\ (x)$. The cause may be that the upstream radius of curvature was confirmed to be dominant in calculating the pressure difference for the Laplace's equation, where radii of curvature in the side view and in the top view are used. The "contact circle model" [**5], which was proposed in the previous paper [8], gives x_1 and x_2 by

$$X_1 = X_u \frac{\cos^2\phi}{1 - \sin\phi}$$

$$X_2 = X_d \frac{\cos^2\phi}{1 + \sin\phi}$$

Substituting these equations into the first term right hand side of Eq. (2) yields

$$2 \cdot \sigma \left(\frac{2}{h} + \frac{1}{R_u} \right) \cdot \left(x_d \frac{\cos^2\phi}{1 + \sin\phi} - x_u \frac{\cos^2\phi}{1 - \sin\phi} \right) \cdot k \cdot h \cdot \tan\phi \qquad (8)$$

where

$$R_u = \frac{\sin\phi}{1 - \sin\phi} x_u$$

2.3.5 Relationship between x_d , x_u , and Projected Bubble Area on the Top View

Downstream interfacial location x_d in Eq.(8) can be expressed based on the "contact circle model" as

[**5] Shape of Liquid-gas interface in the top view can be expressed as the maximum arc which can be put into the passage, i.e., the arc touches the side wall.

$$x_d = (1+\sin\phi)\cdot\left(\frac{x_u}{1-\sin\phi}+\frac{-aR_u+\sqrt{a^2R_u^2-ac\cdot\tan\phi}}{a\cdot\tan\phi\cdot\cos\phi}\right) \tag{9}$$

where

$$a=\left(\frac{90+\phi}{180}\pi\right)\tan\phi+1$$

$$c=\pi R_u{}^2-S$$

2.3.6 Friction Force by a Liquid Flow

As mentioned in subsection 2.3 (4), the friction force can be estimated assuming that velocity profile is the Poiseullie flow. The wall shear stress in a parallel plate with the gap size of *h*, τ_w,can be expressed as

$$\tau_w = 6\mu\frac{u(x)}{h}$$

where *u(x):* average velocity over a cross-sectional area at location *x*

μ : viscosity coefficient of the liquid

The second term on right hand side of Eq.(2), i.e. the friction term, is given by

$$\iint_F \tau_w dF = \iint_F 6\mu\frac{u(x)}{h}dF$$

where

$$dF = 2\tan\phi\cdot x\cdot dx\cdot 2$$

At first, the liquid friction force is expressed for the liquid in the divergent passage as

$$\int\int_F \tau_w dF = \frac{24}{h}\mu\cdot\tan\phi\left(\int_{x_0}^{x_u} xu(x)dx+\int_{x_d}^{x_e} xu(x)dx\right)$$

Making use of the equation of continuity, the second term on the right hand side of Eq.(2) becomes

$$= \frac{24}{h}\mu \cdot \tan\phi \left(\int_{x_0}^{x_u} x_u \frac{dx_u}{dt}\, dx + \int_{x_d}^{x_e} x_u \frac{dx_u}{dt}\, dx \right) = \frac{24}{h}\mu \cdot \tan\phi \times x_u \frac{dx_u}{dt}(x_u - x_0 + x_e - x_d) \qquad (10)$$

Secondary, a friction force outside the passage is taken into account. As a first approximation, the liquid in the outside of the divergent passage is assumed to flow through a hypothetical channel at the same velocity as that at the outlet of the divergent passage and to return to the inlet. From the assumption and the integration, the friction force is given by Eq. (11) instead of Eq. (10).

$$\iint_F \tau_w dF = \frac{24}{h}\mu \cdot \tan\phi \times x_u \frac{dx_u}{dt}(x_u - x_0 + x_e - x_d + x_e - x_0) \qquad (11)$$

Substituting Eqs. (7), (8), (9), and (11) into Eq.(2), an ordinary differential equation with respect to x_u is obtained. The ordinary equation is solved as an initial value problem. This is calculated using the fourth order Runge-Kutta method.

3. ANALYTICAL RESULTS

Initial values are taken as x_u =0.01 m, dx_u/dt=0 m/s in accordance with the authors' experiments. Values of the viscosity coefficient, surface tension, and density at 290 K were referred to literature [11] . After the bubble comes out of the passage, some relationships are not appropriate, thus calculated results are excluded from the results.

3.1 Effect of Friction in the Outside of the Passage

Upstream interface location x_u was calculated in the case of taking the outside friction into account using Eq.(11) and in the case of neglecting the outside friction using Eq. (10), respectively. The results are plotted against time in Fig. 2 for the projected bubble area S of 130 mm^2, gap sizes h of 0.5, 1, and 2 mm, divergent angle ϕ of 2.8 $^\circ$, and effective area ratio k =0.15. It is seen that the former differs from the latter. Hence, it is concluded that the friction in the outside of the passage is not negligible. Therefore, Eq. (11) in stead of Eq. (10) is employed to Eq. (2) from subsection 3.2.

3.2 Effect of the Effective Area Ratio *k*

Figure 3 shows the predicted changes in upstream interface location x_u with time at the divergent angle ϕ of 2.8 $^\circ$, the projected bubble area S of 130 mm^2, and the gap size h of 1 mm for various k =0.1,0.15, and 0.3. It is obvious that the value of k has a strong effect on the bubble behavior. By the authors' other experiment[**6], the value of k was found to be a function of the bubble location, gap size, and divergent angle and took from 0.1 to 0.3. An exact function form of k was not obtained. Hence, the constant value of 0.15 is chosen as k in the following calculations, since it is the average value in the experiment.

3.3 Effect of Projected Bubble Area in the Top View

The calculated upstream interfacial location x_u are shown with time by curves and the measured x_u are reproduced from the previous report[8] by symbols for the gap size h of 1 mm and the divergent angle ϕ of 2.8 $^\circ$ with the projected bubble area S as the parameter in Fig. 4. The upstream interfacial location moves downstream faster, as S becomes greater. The calculated results show the same tendency as measured those. As S becomes greater, the area pressed on the side wall by the bubble; ($k\,h\,(x_2 - x_1) / \cos\theta$) increases. The force by the

[**6] The experimental apparatus was inclined. Forces acting on the bubble were balanced with the buoyancy force, causing the bubble to come to rest. Then, the inclination angle and the bubble location were measured for the stationary state. Substituting the measured data into a force balance equation, an unknown variable, i.e., *k*, was estimated.

bubble acting on the liquid, the first term on right hand side of Eq. (2), is proportional to (x_2 - x_1). Thus, the force increases with projected bubble area. This may be thought to be a primary reason that the bubble moves faster as the bubble projected area increases. The deviations from the experimental results will be described in section 3.5.

3.4 Effect of Gap Size in the Side View

The calculated x_u is shown against time by curves and the measured x_u is reproduced by symbols for ϕ of 2.8 $^\circ$ and S of around 130 mm^2 with gap size h as the parameter in Fig. 5. As seen from the figure, the greater the gap size becomes, the faster the upstream interfacial location moves, and the calculation results correspond to experimental those. As the gap size becomes greater, the unsteady term of Eq. (7) increases, the force by the bubble acting on the liquid, i.e. Eq. (8), becomes higher, and the friction force of Eq. (11) decreases. The reason may be that the changes in Eqs. (8) and (11) are more effective than that in Eq. (7). If the gap size becomes much greater than the present those, the liquid flow is expected not to be negligible in the four corner gaps between the bubble and the inner wall of the divergent passage. An observation showed that the shape for the gas-liquid interface in the side view deviated from an arc as the gap became much greater.

3.5 Effect of Divergent Angle

The calculated x_u are shown against time by curves and the measured x_u are indicated by symbols with divergent angle as the parameter for h of 1 mm and S of around 80 mm^2 in Fig. 6. It is seen that x_u for ϕ of 1° moves faster than that for 2.8° and that calculated x_u is similar to the measured that. The reason is explained as follows: For the constant projected bubble area of around 80 mm^2, an amount of liquid mass in the divergent passage at ϕ of 1° is smaller than that at ϕ of 2.8°. The bubble shape for ϕ of 1° becomes longer than that ϕ of 2.8° at the constant projected bubble area, and thus the force by the bubble acting on the liquid for ϕ of 1°, the second term on the hand of the Eq. (2), becomes greater.

From sections 3.3 to 3.5, the present analysis can predict the effect of the gap size, projected bubble area, and divergent angle on the measured bubble behavior for the previous paper within a certain precision. Hence, it is confirmed that the fluid mechanics of the bubble behavior, described in the present paper, is appropriate essentially. However, the analysis did not predict those with enough accuracy as shown in Figs. 4 to 6. The reasons may be as follows: The liquid flows through the four corner gaps between the bubble and the inner were neglected. The friction of outside the passage was not estimated accurately. The ratio of the effective area ratio k was assumed to be constant. The one-dimensional approximation was made. The equation for the friction force was derived from the steady laminar flow. The fiction between the liquid and the side wall was neglected. Other friction forces and drag forces were not taken into account. Thus, those must be estimated precisely to improve the accuracy of the calculation. In the case that the contact angle is not zero, it is considered that the present model is not applicable directly to the case, and thus further studies are needed.

4. CONCLUSIONS

Behavior of a bubble bridging a cross section of a horizontal narrow divergent passage is studied analytically under the Earth gravity condition from the point of view of a basic study for technologies of separating gas and maintaining the liquid under a microgravity condition. The followings are obtained.

(1) Based on the liquid motion instead of the bubble motion, a one-dimensional momentum equation is derived for analyzing the bubble behavior.

(2) The momentum equation is arranged to an ordinary differential equation with respect to one variable x_u, i.e. upstream interface location, using a “contact circle model” which was proposed by the authors.

(3) The present one-dimensional analysis predicts the bubble behavior within a certain precision and explains the effects of the projected area, gap size, and divergent angle on the

bubble behavior which was reported in the previous report.

ACKNOWLEDGMENT

The authors would like to express their thanks to Messrs. Kazuyuki SHIBAHARA, Takao KATOH, and Koji KOBAYASHI, students at Fukui University, for their cooperation in this study.

APPENDIX See Fig. 7

REFERENCES

(1) Fujii, T. and Ohta, J., *Lecture Series for Japan Society of Multiphase Flow*, No.5, (1990), pp. 63-85. (in Japanese)

(2) Furukawa, M., Ishii, Y., Miyazaki, Y., Iida, T., Report on Power Station System and Thermal Management System in Space (P-SC194) by JSME, (1993) , pp.111-119. (in Japanese).

(3) Batchelor, G.K., *An Introduction to Fluid Dynamics*, Cambridge University Press. (1967).

(4) Ichikawa, N., Report on Power Station System and Thermal Management System in Space (P-SC194) by JSME, (1993), pp. 134-144.(in Japanese)

(5) Taylor, G., and Saffman, P. G., *Quart. J. Mech. And Applied Math*. Vol. XII, Pt. 3, (1959) pp. 265-279.

(6) Moriyama, K., Inoue, A., *Trans. of Japan Society of Mechanical Engineers (B),* **59**,560 (1993-4), pp. 1003-1011. (in Japanese)

(7) Imai, R., Yano, T., Enya, S., *Trans. of Japan Society of Mechanical Engineers (B),* **60**, 560 (1994), pp. 1242-1249. (in Japanese)

(8) Ohta, J., Fujii, T., Koketsu, M., Yamamoto, F., *Trans. of Japan Society of Mechanical Engineers (B),* **61**, 581, (1995), pp.201-207. (in Japanese) The English version is published in “Heat Transfer Japanese Research”.

(9) Landau, L.D. and Lifschits, E.M., *Fluid Mechanics*, Adison-Welsley, (1960).

(10) Weislogel, M. M. and Ross, H. D., *Micrograv. Sci. Tech.*Ⅲ-1, (1990), pp.25-32.

(11) JSME, JSME data book: *Thermophysical Properties of Fluids*, (1991), pp. 22-23.

FIGURE LIST

Fig.1 Explanation of effective area pressed against side wall. A black ellipse denotes an area of a bubble presses against side wall. An effective area ratio *k* is defined as that of the black ellipse to the gray rectangular between x_1 and x_2

Fig. 2 Calculated upstream location vs. time. Friction for outside of the divergent passage has a strong effect on the bubble behavior.

Fig. 3 Calculated upstream location vs. time. Value of the effective area ratio has a strong effect on the bubble behavior.

Fig. 4 Calculated upstream location vs. time (effect of projected bubble area on the top view). Analytical results are compared with experimental those (the authors' previous report [8]). The former corresponds to the latter

Fig. 5 Calculated upstream location vs. time (effect of gap size). Analytical results are compared with experimental those (the authors' previous report [8]). The former is similar to the latter.

Fig. 6 Calculated upstream location vs. time (effect of divergent angle). Analytical results are compared with experimental those. The former is similar to the latter.

Fig. 7 Experimental apparatus (with side passage) [8]

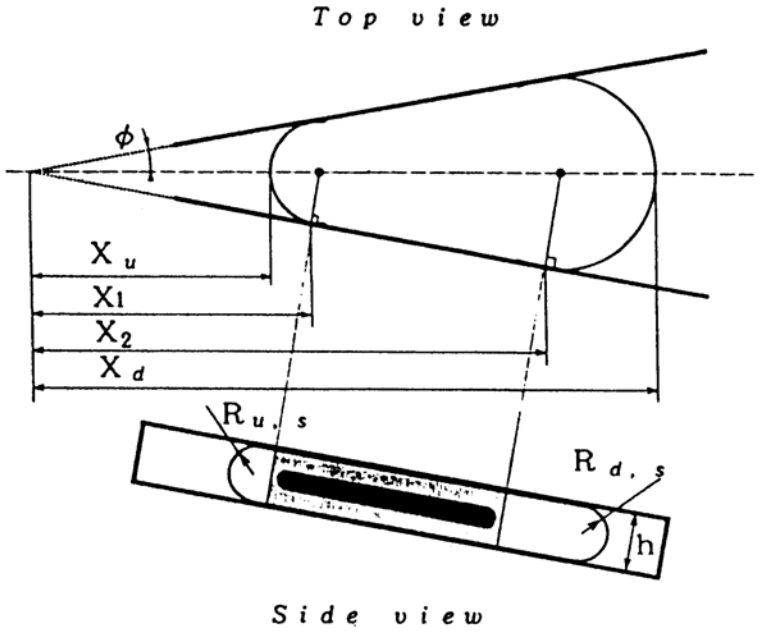
Top view
ϕ
X u
X1
X2
X d
R u, s
R d, s
h
Side view

Fig. 1

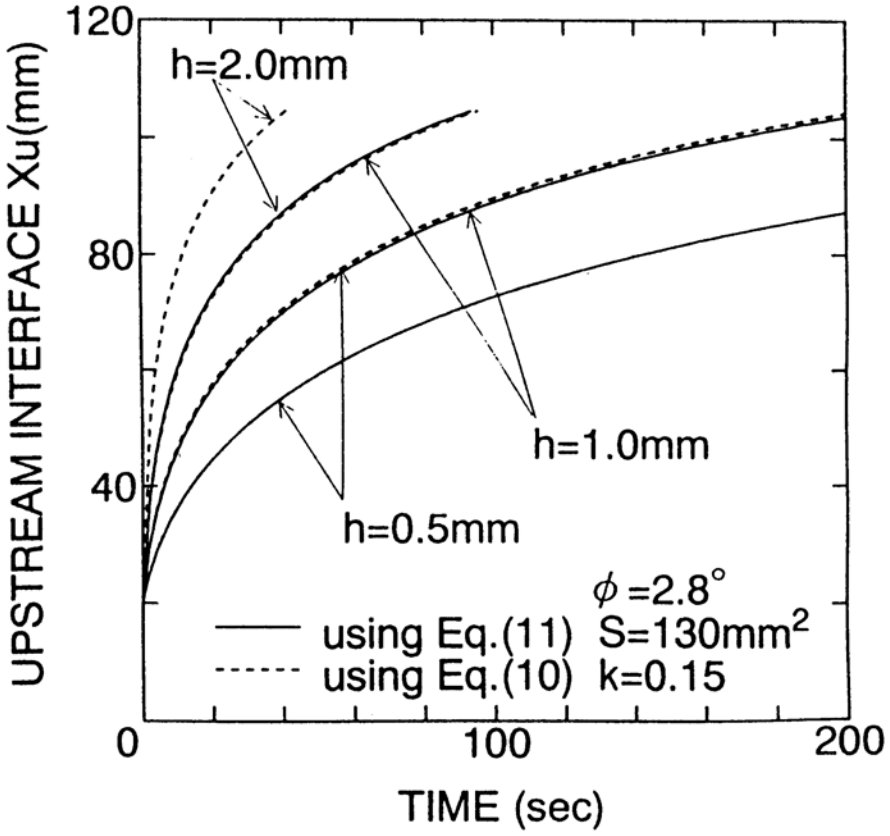
120
80
40
0
100
200
UPSTREAM INTERFACE Xu(mm)
TIME (sec)
h=2.0mm
h=1.0mm
h=0.5mm
ϕ =2.8°
using Eq.(11) S=130mm²
using Eq.(10) k=0.15

Fig. 2

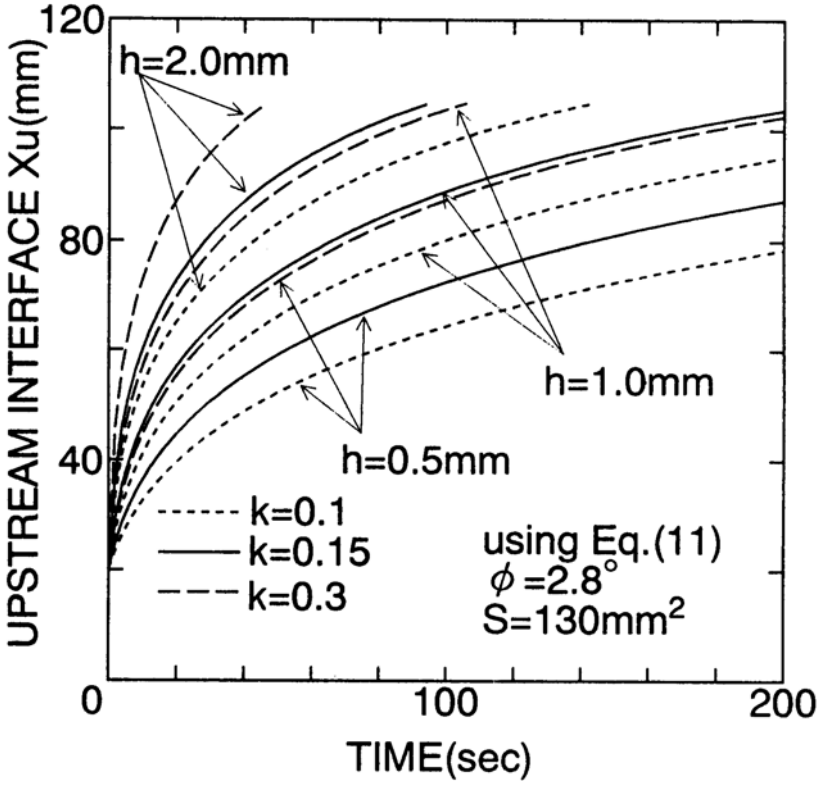
h=2.0mm
h=1.0mm
h=0.5mm
k=0.1
k=0.15
k=0.3
using Eq.(11)
ϕ =2.8°
S=130mm²
UPSTREAM INTERFACE Xu(mm)
TIME(sec)
120
80
40
0
100
200

Fig.3

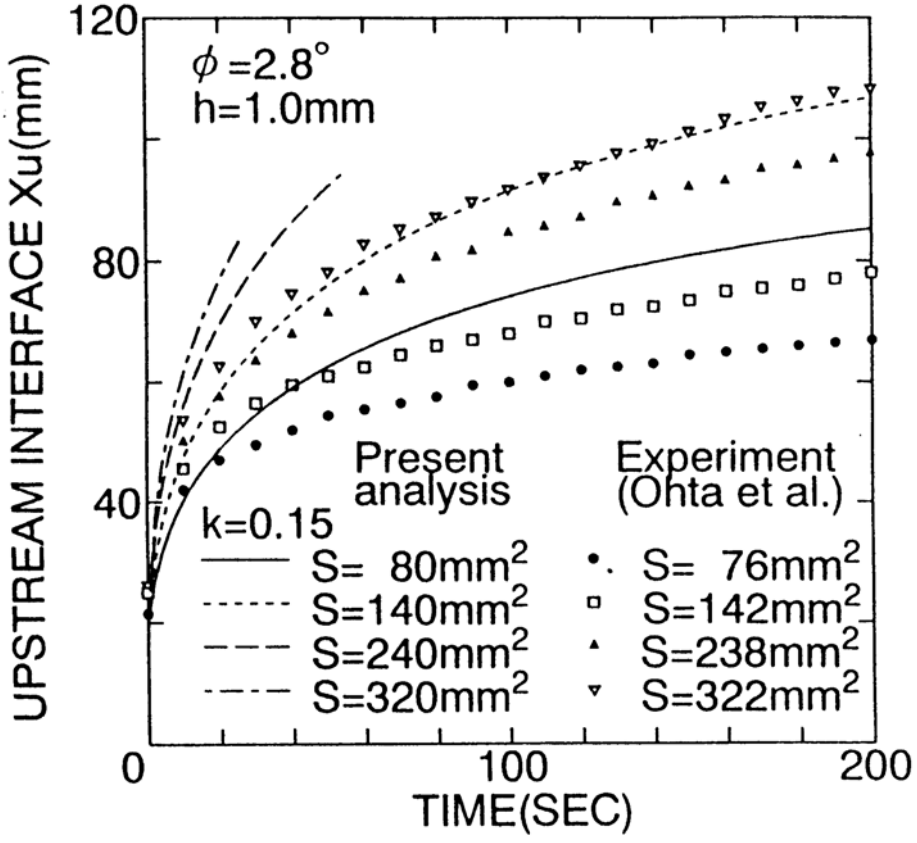
ϕ =2.8°
h=1.0mm
Present analysis
Experiment (Ohta et al.)
k=0.15
S= 80mm²
S=140mm²
S=240mm²
S=320mm²
S= 76mm²
S=142mm²
S=238mm²
S=322mm²
UPSTREAM INTERFACE Xu(mm)
TIME(SEC)
120
80
40
0
100
200

Fig.4

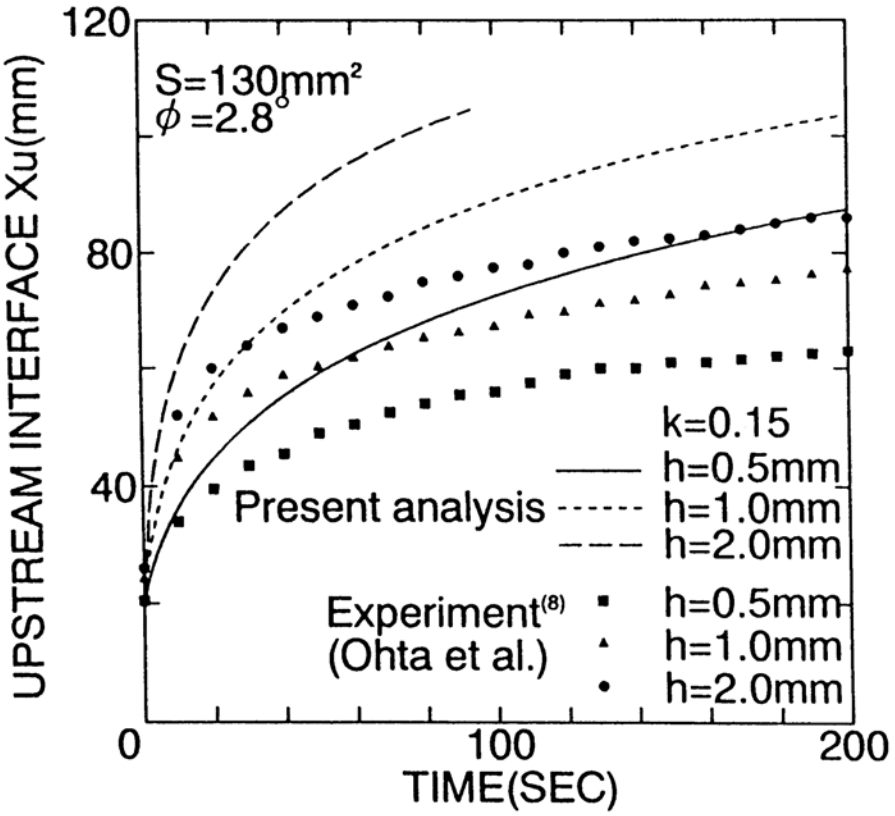
S=130mm²
φ=2.8°
k=0.15
h=0.5mm
h=1.0mm
h=2.0mm
Present analysis
Experiment(8)
(Ohta et al.)
h=0.5mm
h=1.0mm
h=2.0mm
UPSTREAM INTERFACE Xu(mm)
TIME(SEC)
0
40
80
120
100
200

Fig.5

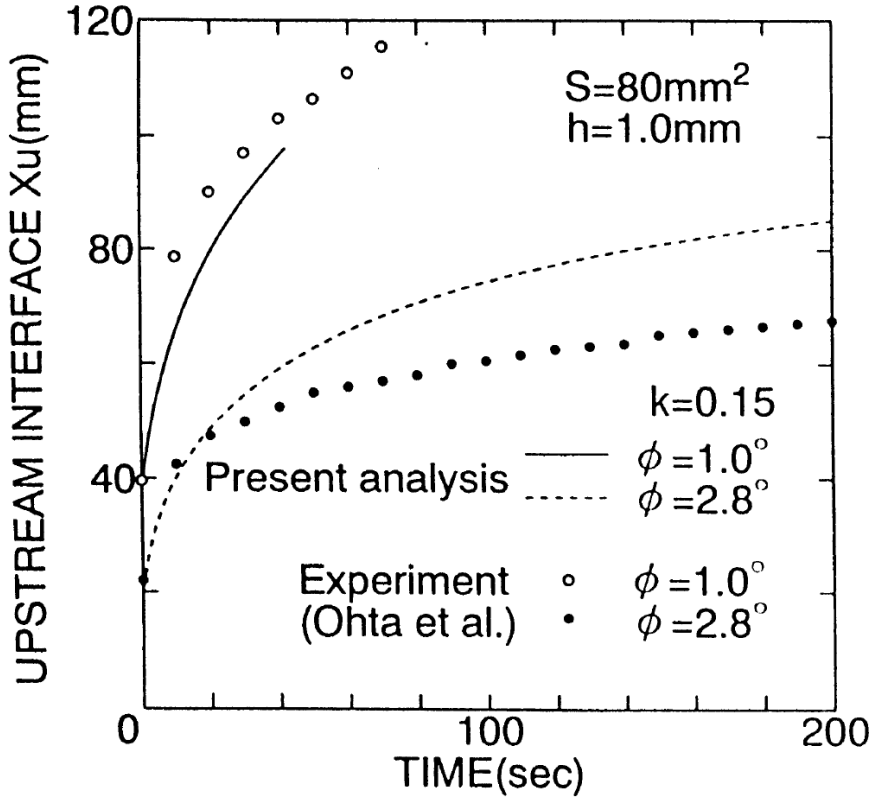
S=80mm²
h=1.0mm
k=0.15
φ=1.0°
φ=2.8°
Present analysis
Experiment
(Ohta et al.)
φ=1.0°
φ=2.8°
UPSTREAM INTERFACE Xu(mm)
TIME(sec)
0
40
80
120
100
200

Fig.6

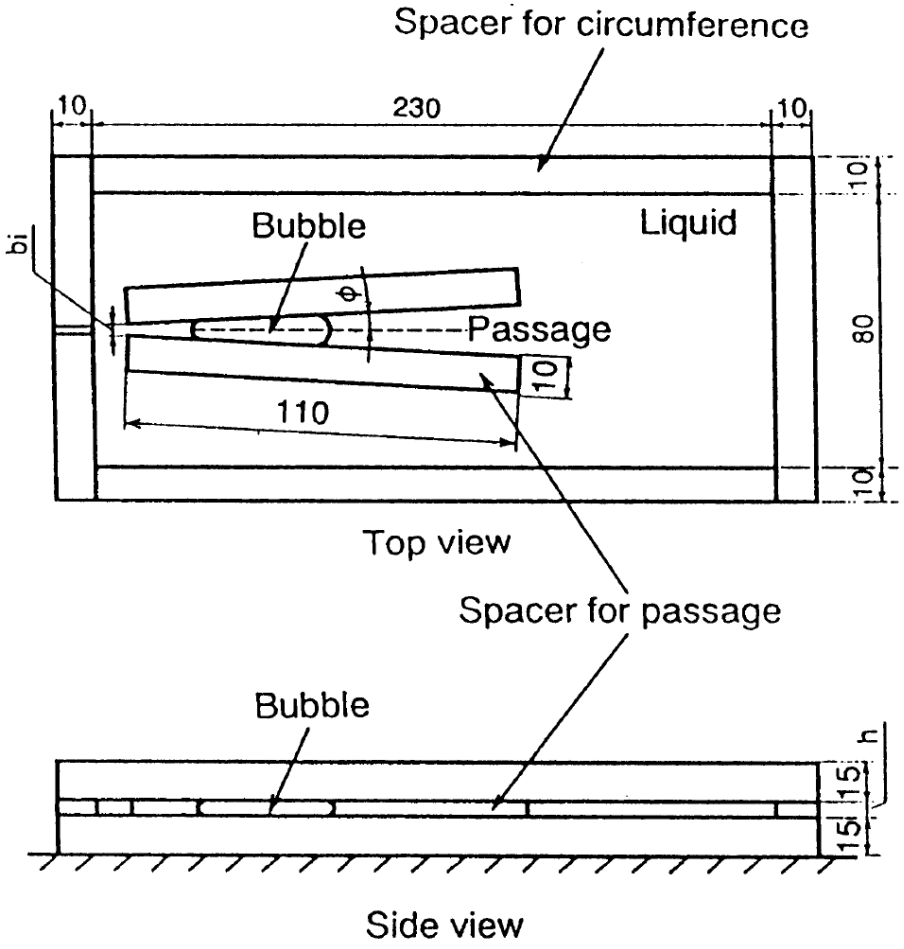
Spacer for circumference
10
230
10
10
Bubble
Liquid
bi
ϕ
Passage
80
10
110
10
Top view
Spacer for passage
Bubble
h
15
15
Side view

Fig.7